Int J Adv Manuf Technol (2016) 84:1769–1776
DOI 10.1007/s00170-015-7863-y

ORIGINAL ARTICLE

# Studies on the spatter behaviour when welding AA5083 with a Yb-fibre laser

**Baohua Chang**[1,2] · **Jon Blackburn**[1] · **Chris Allen**[1] · **Paul Hilton**[1]

Received: 29 April 2015 / Accepted: 13 September 2015 / Published online: 21 September 2015


**Abstract** The processing advantages of welding with high brightness and 1 μm wavelength laser sources have been well reported. However, it is also reported that such high brightness laser sources, whilst providing the necessary penetration depth and welding speed, may result in unacceptable levels of weld spatter. So far, the effects of process parameters on spatter formation have not been well studied on aluminium alloys. In this paper, systematic experimental trials were carried out on the AA5083 aluminium alloy plates to study the effects of different process parameters on the spatter generated. High speed imaging and numerical modelling (using the computational fluid dynamic, CFD) were used to understand the formation mechanisms of the spatter. Results show that the process parameters having the most influence on spatter formation are laser power, welding speed × focal length of the focusing unit, laser power squared × welding speed, laser power squared × focal length of the focusing unit. The welding process in aluminium alloy AA5083 aluminium alloy is quite unstable, the occurrence of spatter ejections is closely related to the turbulence in the melt pool, and full penetration welds tend to produce less spatter than partial penetration welds. To minimise spatter ejection, it is recommended that a high welding speed is used with the laser power just sufficient to achieve full penetration the joint geometry, and the focus position of the laser beam should be appropriately away from the top surface of the workpiece.

✉ Baohua Chang
bhchang@tsinghua.edu.cn

[1] TWI Ltd, Granta Park, Great Abington, Cambridge CB21 6AL, UK

[2] State Key Laboratory of Tribology, Department of Mechanical Engineering, Tsinghua University, Beijing 100084, People's Republic of China

**Keywords** Laser welding · Aluminium alloys · Spatter · Computational fluid dynamics (CFD) · High speed imaging

## 1 Introduction

The beam quality of solid-state laser sources using either thin disc or fibre technology is significantly better than that of Nd:YAG rod laser sources. As a result, the light can be focused into smaller diameter beam widths and hence to higher power densities. The principal processing advantage of these laser sources (i.e. Yb-fibre and Yb:YAG disc) in welding is their ability to provide a substantial increase in either penetration depth or welding speed at a given laser power[1–9].

However, it is also reported that these laser sources, whilst providing the necessary penetration depth and welding speed, may result in unacceptable levels of weld spatter, which is characterised here as the ejection of melt from the process[10, 11]. Despite the obvious effect on surface appearance, and resulting fit-up issues for subsequent assembly operations, the loss of material through weld spatter and the associated instability in the process may also result in other imperfections/defects, such as underfill and undercut. Consequently, there is an industrial need, for current and future adopters of high brightness laser welding, to understand spatter formation mechanism(s) and use appropriate measures/procedures to reduce/eliminate spatter.

Kawahito et al. [12] investigated the occurrence of spatter when laser welding 304 stainless steel with a continuous-wave (cw) IPG YLR-10000(10 kW) fibre laser. The effects of welding speed on spatter formation were investigated. It was found that the spatter was formed when the welding speed was greater than ~10 m/min, and consequently, the weld pool was relatively short. A long weld pool was thought to be effective in reducing the formation of spatter.

Kaplan et al. [13, 14] also studied spatter formation when laser welding 304 stainless steel with a cw IPG YLR-15000 (15 kW) fibre laser. The effects of laser power, welding speed, and focus position on spatter formation were examined. It was observed that at a laser power of 15 kW, with a focus position at or above the top surface of the workpiece, a vertically upward flowing column of molten material periodically formed behind the keyhole and subsequently broke into large escaping droplets of molten metal (i.e. spatter). A focus position below the top surface of the workpiece increased the size of the keyhole, which was observed to reduce the occurrence and size of the spatter. At approximately half the power (and welding speed), it was noted that a more stable melt environment was created around the keyhole, which led to a significant reduction in the amount of spatter generated.

Although research has been performed on spatter formation during the laser welding with fibre laser sources, the majority of the work has focused on stainless steels. The studies on the effects of process parameters on spatter on other materials are very limited, such as aluminium-based alloys [15–17].

This research set out to study spatter formation when laser welding a common aluminium alloy (AA5083), with a 1-μm wavelength, fibre laser source. The work was targeted at understanding the key parameters and mechanisms which result in spatter formation and providing practical guidelines to reduce/eliminate spatter when welding the aluminium alloy with high brightness fibre/disc lasers.

## 2 Experimental approach

Aluminium alloy AA5083 plate of 4 mm thick was used, with the chemical composition listed in Table 1. The plates were cut into rectangular test pieces of approximately 150× 300 mm. Argon was used as a shielding gas. In all instances, the argon gas used was to a purity of 99.998 %.

All trials were performed using an IPG Photonics YLS-5000 (5 kW) Yb-fibre laser, of output wavelength 1070± 10 nm. Table 2 details the collimating and focusing units used and the resulting calculated laser beam profile characteristics. For all the trials performed, the process head was mounted to a 6-axis articulated arm Kawasaki FS-060 robot. A Phantom 7 high-speed camera was used during selected trials to observe the keyhole and weld pool behaviour. A Cavitar HF diode laser (808 nm wavelength) was used to illuminate the process.

**Table 1** Chemical composition of the aluminium alloy AA5083 aluminium alloy plates used

| Elements | Si | Fe | Cu | Mn | Mg | Zn | Ti | Cr | Al |
|---|---|---|---|---|---|---|---|---|---|
| % | 0.4 | 0.4 | 0.1 | 0.4 | 4.0 | 0.25 | 0.15 | 0.05 | Balance |

**Table 2** Optic combinations and process parameters used in the BoP melt run and high speed imaging trials

| Parameters | Values |
|---|---|
| Delivery fibre core diameter, mm | 0.15 |
| Beam parameter product, mm·mrad | 6 |
| Collimating unit focal length, mm | 160 |
| Focusing unit focal length, mm | 160 |
| Beam width, mm | 0.15 |
| Rayleigh length, mm | 0.94 |
| Laser power, kW | 2, 3, 4, 5 |
| Welding speed, m/min | 1, 3.5, 5, 8 |
| Focus position, mm | −4, −2, −1, 0, +2, +4 |

## 3 Scope of work

The scope of work was performed in four distinct phases:

a. Firstly, systematic BoP (bead on plate) melt run trials, to simulate a close fitting butt joint, were carried out to study the influence of key process parameters (laser power and welding speed) on spatter during laser welding. The spatter generated was collected from the workpiece after welding and weighed using an electronic balance. These results were then statistically analysed using response surface methodology (RSM). The parameters, and their ranges, examined are also listed in Table 2.
b. Secondly, high speed imaging was used to investigate the keyhole and weld pool behaviour and the occurrence of spatter in selected trials on AA5083 aluminium alloy plates.
c. Thirdly, numerical modelling was performed for laser welding of AA5083 aluminium alloy, using the computational fluid dynamic (CFD) software Fluent, to study the effects of key parameters on characteristics of fluid flow fields. More details of the CFD model can be found in a previously published paper [18].
d. Finally, computational predictions concerning the fluid flow characteristics in weld pool were analysed in combination with the actual spatter levels measured and the spatter behaviour observed in the experiments. The relationships between spatter and fluid flow features within the weld pool were examined.

## 4 Results and discussion

### 4.1 Experimental trials and statistical analysis

A total of 35 BoP melt run trials were performed with focus position, at −1 mm (i.e., the beam width was positioned 1 mm

**Table 3** Spatter weight and penetration state for different laser welding parameters

| BoP No. | Laser power, kW | Welding speed, m/min | Spatter weight, g | Penetration |
|---|---|---|---|---|
| 1 | 4 | 1 | 0.0711 | Full |
| 2 | 4 | 5 | 0.0066 | Full |
| 3 | 4 | 8 | 0.0059 | Full |
| 4 | 2 | 3.5 | 0.0177 | Partial |
| 5 | 2 | 5 | 0.0108 | Partial |
| 6 | 2 | 8 | 0.0021 | Partial |
| 7 | 3 | 3.5 | 0.0119 | Full |
| 8 | 3 | 5 | 0.0193 | Full |
| 9 | 3 | 8 | 0.0075 | Intermittent full |
| 10 | 5 | 3.5 | 0.0337 | Full |
| 11 | 5 | 5 | 0.0386 | Full |
| 12 | 5 | 8 | 0.0035 | Full |
| 13 | 4 | 3.5 | 0.0124 | Full |
| 14 | 4 | 8 | 0.0016 | Full |

below the top surface of the workpiece) and the inert gas shielding flow rate at 30 L/min. The results of those trials, detailed in Tables 3, were analysed statistically. Various parameter combinations resulted in partial, intermittent full, and full penetration. No direct correlation between the penetration state and the weight of spatter collected was observed. The input variables used in the statistical analysis were:

A. Laser power (kW)
B. Welding speed (m/min)
C. Focal length of the focusing unit (mm)

The statistical analysis indicated that a cubic model provided the most complete description of the response. Linear regression analysis and a backward elimination technique were used to remove non-significant terms from the quadratic model. The *p* values, or statistical significance, of individual terms were determined using analysis of variance (ANOVA) techniques. Those terms with *p* values >0.10 were deemed statistically insignificant and removed from the model. Table 4 details the terms, and their *p* values, included in the model. The significant input variables, within the ranges evaluated, were:

A: Laser power
BC: Welding speed × focal length of the focusing unit
$A^2B$:Laser power$^2$ × welding speed
$A^2C$:Laser power$^2$ × focal length of the focusing unit

Figure 1 shows the influence of laser power and welding speed. Included on the response surface graphs are the measured data points from the experimental trials. This gives an indication of the accuracy of the statistical model. From Fig. 1 and Table 3, it can be seen that weld spatter was minimised by adopting a relatively fast (~8 m/min) welding speed, and the model indicated that high levels of spatter were produced

**Table 4** ANOVA for AA5083 aluminium alloy trials

| Source | Sum of squares | df | Mean square | F value | *p* value, prob>F |
|---|---|---|---|---|---|
| Model | 27.57 | 9 | 3.06 | 8.40 | <0.0001 |
| A: Laser power | 3.59 | 1 | 3.59 | 9.83 | 0.0043 |
| B: Welding speed | 0.31 | 1 | 0.31 | 0.85 | 0.3643 |
| C: Focusing optic | 0.039 | 1 | 0.039 | 0.11 | 0.7456 |
| AB | 0.069 | 1 | 0.069 | 0.19 | 0.6665 |
| AC | 0.97 | 1 | 0.97 | 2.66 | 0.1153 |
| BC | 5.65 | 1 | 5.65 | 15.49 | 0.0006 |
| $A^2$ | 0.0081 | 1 | 0.0081 | 0.022 | 0.8824 |
| $A^2B$ | 6.23 | 1 | 6.23 | 17.08 | 0.0004 |
| $A^2C$ | 3.12 | 1 | 3.12 | 8.54 | 0.0073 |
| Residual | 1.19 | 25 | 0.2 | | |
| Cor Total | 36.68 | 34 | | | |

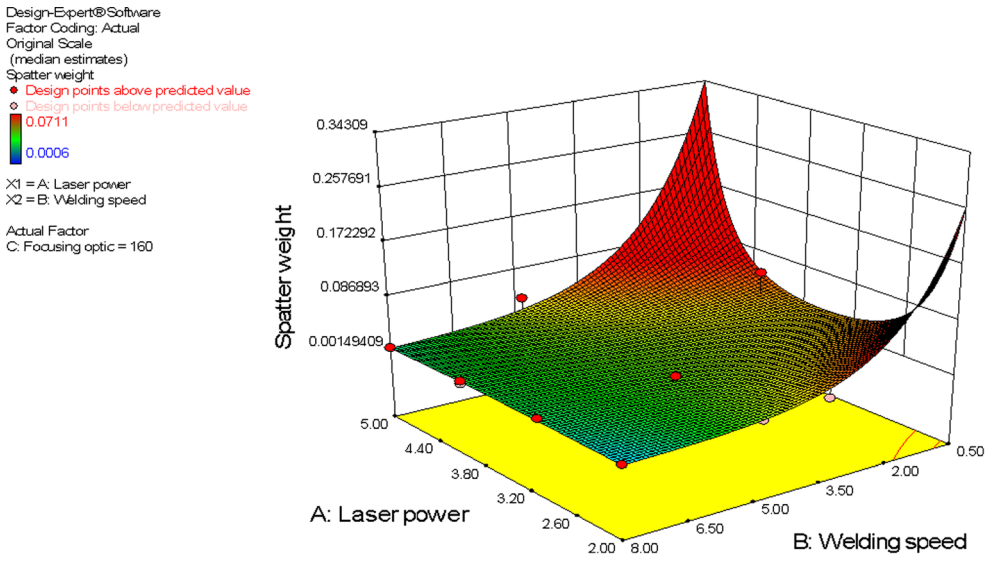


**Fig. 1** Response surface plots, detailing the effects of laser power and welding speed on the resultant spatter weight

when low welding speeds were used with either relatively low or high laser powers.

## 4.2 High speed imaging

The effects of key parameters (welding speed, laser power and focus position) on the keyhole and weld pool behaviour were observed. In addition, a basic quantitative comparison of the spatter ejections has been made by counting the occurrence of spatter ejection from the process for a constant welding distance of 7.5 mm, which are detailed in Table 5. Through the observations, it was found that the no stable keyhole was observed in any of the videos taken, and the keyhole was frequently observed to form and then collapse.

### *4.2.1 Welding speed*

The welding speed was varied between 1 and 8 m/min, and the laser power and focus position were kept constant at 2 kW and 0 mm, respectively. From the high speed videos (see Fig. 2), it was observed that an increase in the welding speed from 1 to 3.5 m/min led to a decrease in the length and width of the weld pool. Further increases in the welding speed from 3.5 to 8 m/min led to a decrease in the width of the weld pool only. A decrease in spatter dimensions was observed as the welding

**Table 5** Process parameter combinations examined to observe, with a high speed imaging system, the spatter formation, weld pool and keyhole

| BoP No. | Laser power, kW | Welding speed, m/min | Focus position, mm | Penetration state | No. of spatter ejections observed | Spatter frequency, $s^{-1}$ |
|---|---|---|---|---|---|---|
| 1 | 2 | 1.0 | 0 | Full | 195 | 433 |
| 2 | 2 | 3.5 | 0 | Intermittent full | 54 | 419 |
| 3 | 2 | 5.0 | 0 | Partial | 44 | 488 |
| 4 | 2 | 8.0 | 0 | Partial | 38 | 675 |
| 5 | 5 | 3.5 | 0 | Full | 62 | 482 |
| 6 | 5 | 5.0 | 0 | Full | 48 | 533 |
| 7 | 5 | 8.0 | 0 | Full | 32 | 569 |
| 8 | 2 | 3.5 | 0 | Intermittent full | 54 | 419 |
| 9 | 3 | 3.5 | 0 | Full | 44 | 342 |
| 10 | 4 | 3.5 | 0 | Full | 45 | 350 |
| 11 | 5 | 3.5 | 0 | Full | 62 | 482 |
| 12 | 5 | 3.5 | −4 | Full | 26 | 202 |
| 13 | 5 | 3.5 | −2 | Full | 44 | 342 |
| 14 | 5 | 3.5 | 0 | Full | 62 | 482 |
| 15 | 5 | 3.5 | +2 | Full | 48 | 373 |
| 16 | 5 | 3.5 | +4 | Full | 53 | 412 |

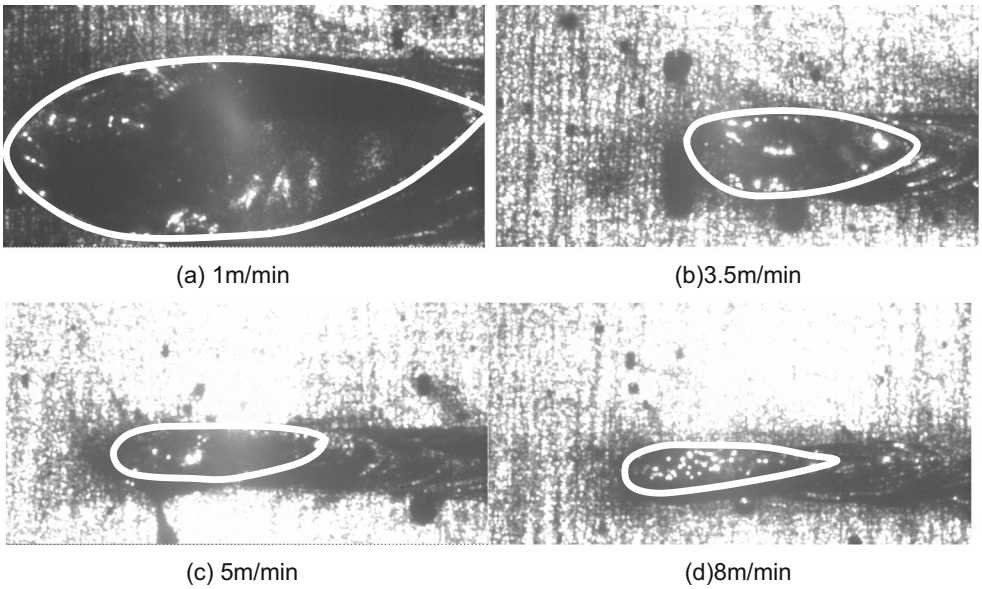


**Fig. 2** Weld pool morphologies produced for different welding speed (with a focus position of 0 mm, and a laser power of 2 kW)

speed increased (note the round particles of different sizes on both sides of a melt run). The number produced per unit time (i.e. spatter frequency) increased with an increase in the welding speed, while the number of spatter ejections over the observed length of workpiece (7.5 mm) decreased as a result of the shorter welding time for increased welding speed.

*4.2.2 Laser power*

The laser power was varied between 2 and 5 kW, and the welding speed and focus position were kept constant at 3.5 m/min and 0 mm, respectively. From the high speed videos (see Fig. 3), it was observed that a laser power of 2 kW resulted in partial penetration in the 4 mm thickness AA5083 aluminium alloy plate. An increase in the laser power to 3 kW resulted in full penetration but decreased the dimensions of the weld pool. The weld pool was less turbulent when full penetration was achieved at 3 kW, but a further increase in the laser power led to an increase in the observed turbulence and a corresponding increase in the number (also the frequency) of spatter ejections from the weld pool. The change in spatter size with laser power was not notable.

*4.2.3 Focus position*

The focus position was varied between −4 and +4 mm, and the welding speed and laser power were kept constant at 3.5 m/min and 5 kW, respectively. From the observation with high

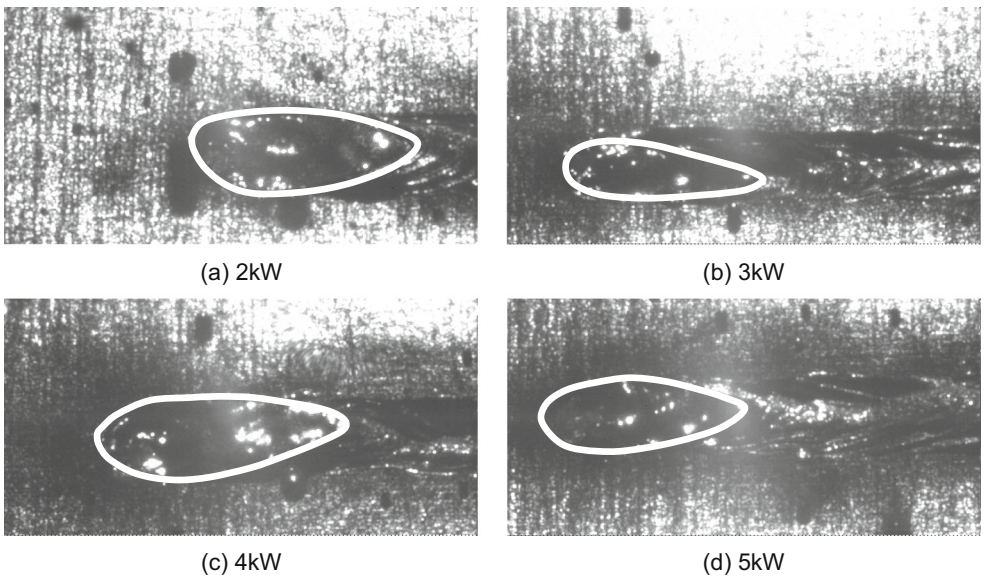


**Fig. 3** Weld pool morphologies produced for different laser power (with a focus position of 0 mm, a welding speed of 3.5 m/min)

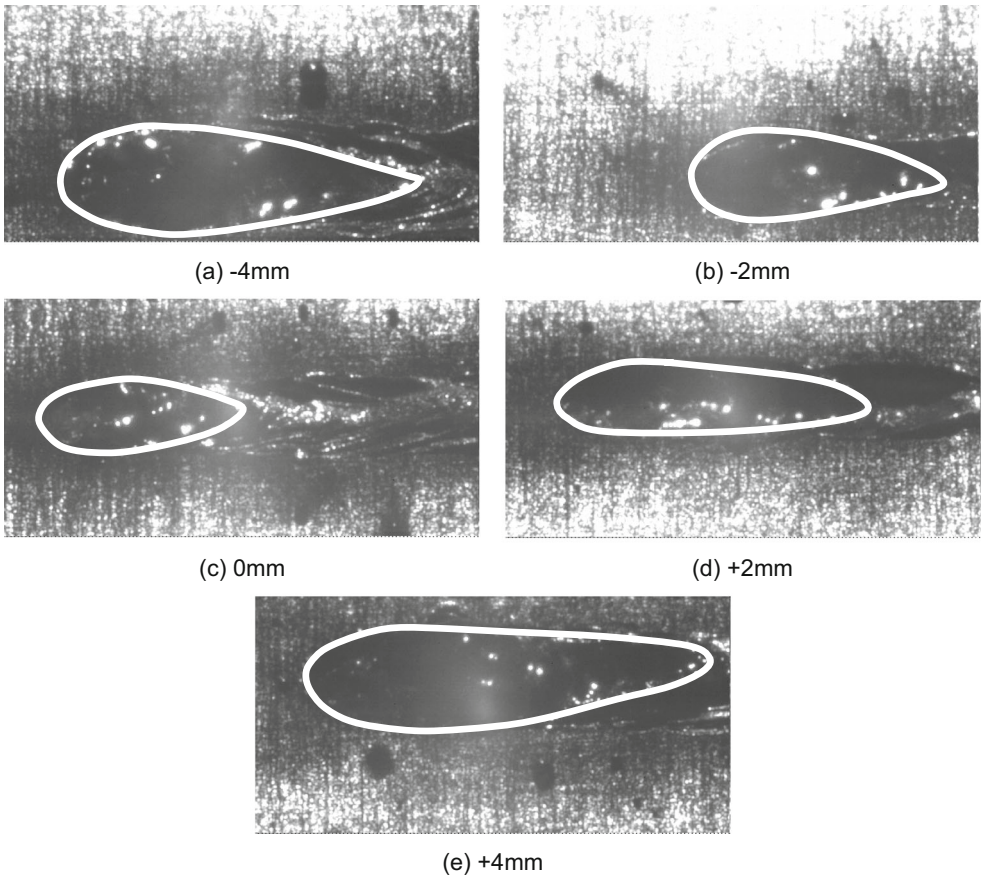


**Fig. 4** Weld pool morphologies produced for different focus positions (with a welding speed of 3.5 m/min and laser power of 5 kW)

speed video, it was found that a large number of spatter ejections occurred with a focus position of 0 mm, which was evident in Fig. 4c where quite a few spatter particles could be seen. Focus positions of −2 or +2 mm decreased the number of spatter ejections compared with a focus position of 0 mm (as provided in Table 5), which was also demonstrated by less spatter particles and cleaner surfaces of workpiece shown in Fig. 4b, d, respectively. Moving the focus position from +2 to +4 mm slightly increased the number of spatter ejections. In contrast, moving the focus position from −2 to -4 mm decreased the number of spatter ejections notably, as in Table 5. Focus positions of −4 and +4 mm resulted in wider and longer weld pools and spatter of larger dimensions, as shown in Fig. 4a, e, respectively.

### 4.3 Numerical modelling

Numerical modelling was carried out for a number of welding conditions, and the maximum velocities and vorticity magnitudes within the weld pools obtained for various welding parameters were shown in Figs. 5, 6 and 7.

The effects of welding speed are shown in Fig. 5. It can be seen that for a given laser power (2 kW), the maximum velocity and vorticity magnitudes in the weld pool increased with increasing welding speed. Figure 6 shows the influence of laser power. For a given welding speed (3.5 m/min), increasing the laser power from 2 to 4 kW decreased the maximum velocities (the penetration depth increases from partial penetration to full penetration). A further increase in the laser power to 5 kW increased the velocities of the weld pool. Figure 7 shows the effects of beam width. It can be seen that the maximum velocity magnitudes within the weld pools decreased when the larger spot size was used, whether the welds were full (5 kW) or partial (2 kW) penetration.

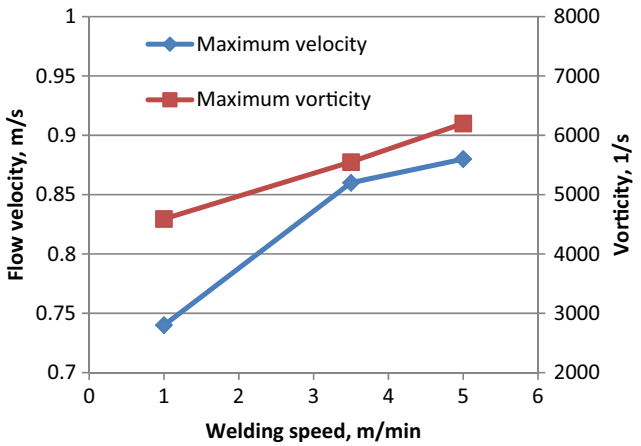


**Fig. 5** Effects of laser welding speed on maximum velocity and vorticity magnitudes in weld pools (laser power: 2 kW)

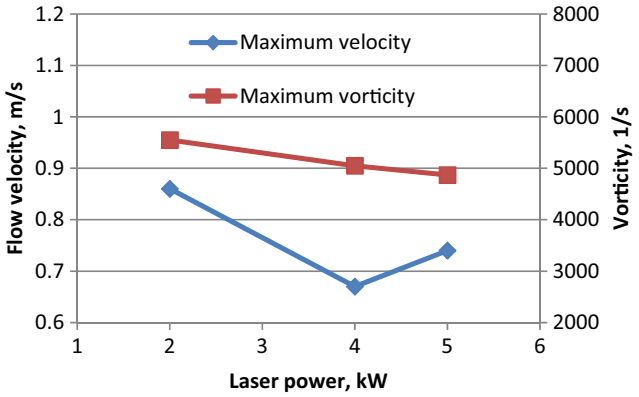


**Fig. 6** Effects of laser power on maximum velocity and vorticity magnitudes in weld pools (welding speed: 3.5 m/min)

## 5 Discussion

Comparing the numerical results in Section 4.3 with the experimental results discussed in Sections 4.1 and 4.2, some correlations can be found between the computations and the previously observed experimental phenomena.

For increased welding speeds, the increase in the turbulence in weld pools, as indicated by the increased fluid velocities and vorticities in Fig. 5, will lead to a larger number of spatter per unit time (i.e. higher spatter frequency). However, the dimensions of the spatter are reduced, which are the same as those of weld pools (Fig. 2), and the total number of spatter ejection, as listed in Table 5, are decreased due to the shorter welding duration; as a result, the metal loss due to spatter ejections are decreased as shown in Fig. 1. Therefore, a high welding speed is preferred to minimize spatter, with other quality requirements being satisfied.

In the present setting, increasing laser power will first make the weld transfer from partial penetration to full penetration (Tables 3 and 5). Such a change in penetration state will lead to a less unstable fluid flow in the weld pool, as indicated by the decreased fluid velocity and vorticity given in Fig. 6, which is also proved by the decreased spatter times listed in Table 5. Meanwhile, the dimensions of both the weld pool and the spatters become smaller. Consequently, the metal loss (i.e. the measured spatter weight) will decrease when the full penetration state is just achieved. After this, a further increase in laser power will result in larger fluid flow velocity, spatter frequency and spatter size, which in turn result in an increased metal loss. Therefore, to minimize spatter, a laser power is recommended just sufficient to achieve the full penetration.

Increasing the brightness of the laser beam, by using a smaller diameter beam width or letting focus located at the top surface (ie without defocusing), will increase the velocity and vorticity in the melt pool (shown in Fig. 7). Under such conditions, the fluid flow in the melt pool is more unstable and hence may cause more spatter ejections (Table 5, BoP No.14). In contrast, when the beam width is increased or the beam is defocused to a small amount (±2 mm in this study), the power density of laser beam at the top surface will decrease, and the velocity and vorticity in the weld pool will decrease as a result (shown in Fig. 7). The number of spatter ejection decreases, thanks to the less unstable weld pool under such conditions (Table 5, BoP No.13 and No.15). Letting focus further into the workpiece (i.e. −4 mm defocusing) results in even less spatter (Table 5, BoP No.12), while letting the focus further away from the workpiece (+4 mm defocusing) leads to more spatter (Table 5, BoP No.16). Although theoretically these two cases should have equal power densities at the top surface, the power density distributions within the keyhole are different, which will result in keyholes and weld pools with different stability and in turn different spatter behaviour. It seems a −4 mm defocusing can generate a more stable keyhole than a +4 mm defocusing. Due to the absent of keyhole in the present CFD model, such effects are not investigated in this work and will be addressed later.

From above analyses, it can be found that the occurrence of spatter ejections is closely related to the turbulence, in terms of flow velocity and vorticity, in the melt pool. The CFD model can be a useful tool in understanding spatter formation mechanisms and explaining influences of welding parameters on spatter behaviour. However, although these correlations are noted, it should be remembered that, being an initial approximation for the spatter study, the present numerical model did not take into account a keyhole. Further development in the numerical modelling approach to incorporate a dynamic

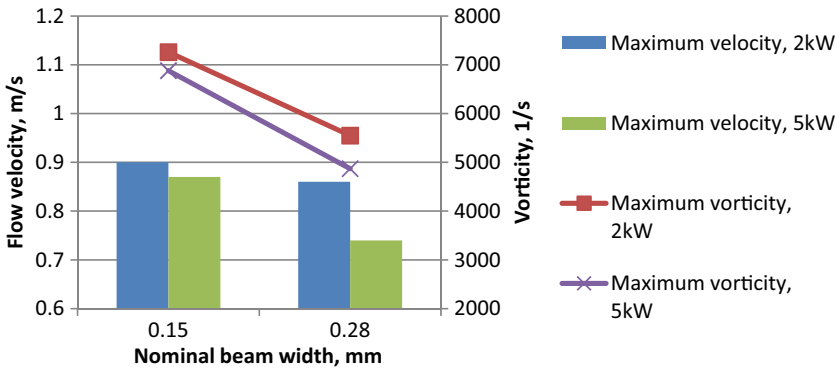


**Fig. 7** Effects of nominal beam width on maximum velocity and vorticity magnitudes in weld pools

keyhole would provide more accurate information and be more helpful in analysing spatter behaviour.

## 6 Conclusions

The following conclusions have been drawn from the work programme detailed above:

- Laser welding trials on 4 mm thickness AA5083 aluminium alloy plate, and subsequent statistical analysis of the results, have indicated that the process parameters having the most influence on spatter formation are laser power, welding speed × focal length of the focusing unit, laser power squared × welding speed, laser power squared × focal length of the focusing unit.
- The laser welding process in AA5083 aluminium alloy is unstable, and no stable keyholes have been observed. The occurrence of spatter ejections is closely related to the turbulence, in terms of fluid flow velocity and vorticity, in the melt pool.
- Increasing welding speed results in more unstable fluid flow in weld pool and therefore higher spatter occurrence frequency, but the total number of spatter and the metal loss due to spatter are reduced because of the decreased spatter dimensions and shorter welding time.
- Full penetration welds tended to produce less spatter than partial penetration welds; increasing the laser power too much will lead to increased spatter.
- Letting focus located at the top surface of workpiece generates the most severe spatter, a slight defocusing (±2 mm in this study) will make the melt pool less unstable and result in less spatter ejections.

**Acknowledgments** This work was funded by TWI's Industrial Members as part of its Core Research Programme. In addition, the numerical modelling work reported in this paper was supported by a Marie Curie International Incoming Fellowship with the 7th European Community Framework Programme (Grant No. 253487) and its return phase (Grant No. 919487).

## References

1. Youhei A, Yousuke K, Hiroshi N, Koji N, Masami M, Seiji K (2014) Effect of reduced pressure atmosphere on weld geometry in partial penetration laser welding of stainless steel and aluminium alloy with high power and high brightness laser. Sci Technol Weld Join 19:324–332
2. Chen W, Pal M (2008) Dual-beam laser welding of ultra-thin AA 5052-H19 aluminum. Int J Adv Manuf Tech 39:889–897
3. Zhang C, Li G, Gao M, Yan J, Zeng XY (2013) Microstructure and process characterization of laser-cold metal transfer hybrid welding of AA6061 aluminum alloy. Int J Adv Manuf Tech 68:1253–1260
4. Yan J, Gao M, Li G, Zhang C, Zeng XY, Jiang M (2013) Microstructure and mechanical properties of laser-MIG hybrid welding of 1420 Al-Li alloy. Int J Adv Manuf Tech 66:1467–1473
5. Ren D, Liu L, Li Y (2012) Investigation on overlap joining of AZ61 magnesium alloy: laser welding, adhesive bonding, and laser weld bonding. Int J Adv Manuf Tech 61:1–10
6. Saha DC, Westerbaan D, Nayak SS, Biro E, Gerlich AP, Zhou Y (2014) Microstructure-properties correlation in fiber laser welding of dual-phase and HSLA steels. Mater Sci Eng A-Struct Mater Prop Microst Process 607:445–453
7. Blackburn JE, Allen CM, Hilton PA, Li L, Hoque MI, Khan AH (2010) Modulated Nd:YAG laser welding of Ti-6Al-4V. Sci Technol Weld Join 15:433–439
8. Li SC, Chen G, Zhang M, Zhou Y, Zhang Y (2014) Dynamic keyhole profile during high-power deep-penetration laser welding. J Mater Process Technol 214:565–570
9. Katayama S, Abe Y, Mizutani M, Kawahito Y (2011) Deep penetration welding with high-power laser under vacuum. Trans JWRI 40:15–19
10. You DY, Gao XD, Katayama S (2013) Visual-based spatter detection during high-power disk laser welding. Optics Lasers Eng 54(SI):1–7
11. Biffi CA, Previtali B (2013) Spatter reduction in nanosecond fibre laser drilling using an innovative nozzle. Int J Adv Manuf Tech 66: 1231–1245
12. Kawahito Y, Mizutani M, Katayama S (2007) Investigation of high power fiber laser welding phenomena of stainless steel. Trans JWRI 36:11–15
13. Kaplan A, Westin E, Wiklund G, Norman P (2008) Imaging in cooperation with modeling of selected defect mechanisms during fiber laser welding of stainless steel. Proceeding of 27th International Congress on Applications on Lasers & Electro-Optics (ICALEO), California, USA. 789–798
14. Kaplan AFH, Powell J (2011) Spatter in laser welding. J Laser Appl 23(032005):1–7
15. Kim JK, Lim HS, Cho JH, Kim CH (2008) Bead-on-plate weldability of Al 5052 alloy using a disk laser. J Ach Mat Manuf Eng 28:187–190
16. Liu JW, Rao ZH, Liao SM, Wang PC (2014) Modeling of transport phenomena and solidification cracking in laser spot bead-on-plate welding of AA6063-T6 alloy. Part I-the mathematical model. Int J Adv Manuf Tech 73:1705–1716
17. Liu JW, Rao ZH, Liao SM, Wang PC (2014) Modeling of transport phenomena and solidification cracking in laser spot bead-on-plate welding of AA6063-T6 alloy. Part II-simulation results and experimental validation. Int J Adv Manuf Tech 74:285–296
18. Chang BH, Allen C, Blackburn J, Hilton P (2013) Thermal and fluid flow characteristics and their relationships with porosity in laser welding of AA5083. Phys Procedia 41:478–487